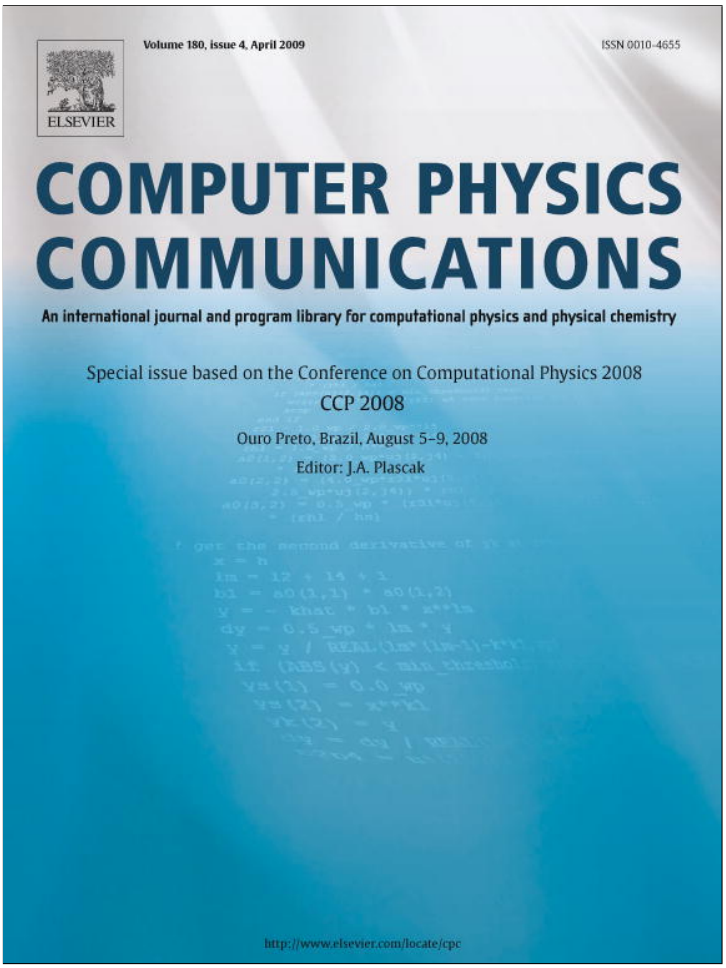

Computer Physics Communications 180 (2009) 636–641

Contents lists available at ScienceDirect

Computer Physics Communications

www.elsevier.com/locate/cpc

Simulations of biomedical atmospheric-pressure discharges

Seung Min Lee [a], Yong Jun Hong [a], Young Sik Seo [a], Felipe Iza [b], Gyoo Cheon Kim [c], Jae Koo Lee [a,*,1]

[a] Department of Electronic and Electrical Engineering, Pohang University of Science and Technology, Pohang 790-784, Republic of Korea
[b] Department of Electronic and Electrical Engineering, Loughborough University, Loughborough, Leicestershire LE11 3TU, United Kingdom
[c] Department of Oral Anatomy, College of Dentistry, Pusan National University, Busan 602-739, Republic of Korea

ARTICLE INFO

Article history:
Received 25 September 2008
Received in revised form 5 January 2009
Accepted 6 January 2009
Available online 8 January 2009

PACS:
52.65.Rr
52.65.Pp
52.80.Pi

Keywords:
Atmospheric-pressure glow discharge
Computer simulation
Energy distribution function

ABSTRACT

The comparison between fluid and particle-in-cell simulation results in different nonthermal helium plasma sources; including an overview of kinds, strengths and limitations of the numerical models is reported. The kinetic information indicates that the electron energy probability function (EEPF) evolves from a three-temperature distribution in RF atmospheric-pressure discharges into a Druyvesteyn type distribution as the driving frequency increases. In microwave helium microplasma, the power delivered to the electrons in the bulk increases, and as a result, the EEPF becomes closer to a Maxwellian distribution. Although the results obtained with fluid models that a Maxwellian energy distribution function are not capable of capturing nonlocal effects in high pressure discharge, the appropriate fluid models will be a good selection to investigate particular problems because of their short simulation time. In addition, since frequent ion–neutral collisions limit the energy acquired by the ions as they transit the sheath, the average ion energy near the electrodes is found to be significantly lowered at atmospheric pressure.

1. Introduction

Atmospheric-pressure discharges have received considerable attention in recent years for their potential economic impact in a broad range of fields. Their nonequilibrium characteristics, chamber-free operation capability, and portability enable new applications of plasmas. Recent research has focused on understanding the production of reactive species, charged particles, and UV photons for bio-medical applications, surface treatments and environmental applications [1–4]. Although the physics of low-temperature nonequilibrium discharges still remains not fully understood, the diagnostics of these atmospheric-pressure plasmas is challenging and limited [5]. In an attempt to overcome the experimental challenges, numerical techniques such as fluid, particle-in-cell and hybrid models are often used to estimate plasma parameters. For example, plasma models can provide detailed electron and ion kinetic information that often is not available experimentally [6–10]. Fluid models are widely used in computational studies of low-temperature discharges because of their short simulation time [11]. However, these models are not capable of capturing nonlocal effects because they infer the velocity distribution from local values of the electric field. Although the high collisionality of atmospheric-pressure discharges favors operation in the local regime, it would be wrong to think that in all atmospheric-pressure plasmas the electrons are in equilibrium with the electric field [6]. Although a kinetic analysis is computationally more demanding than a fluid simulation, kinetic simulations are necessary to validate fluid results and to obtain self-consistent kinetic information not available in fluid models [12,13].

In this study, particle-in-cell Monte Carlo collision (PIC-MCC) simulation results are compared with fluid simulation results. DC, RF and microwave driven helium atmospheric-pressure discharges are considered in the present study. The electron energy probability function (EEPF) can be far from equilibrium and differs substantially from the Maxwellian distribution assumed in the fluid models. This mismatch is the main reason for the differences observed in the predictions made by the two models.

This manuscript is arranged as follows. In Section 2, a brief description of the numerical models with their capabilities and limitations, and the discharge conditions used in the study are presented. A comparison between the simulation results obtained with different models is discussed in Section 3. A symmetrical parallel plate and an asymmetric coaxial configuration are considered in the study. Additionally, some aspects of the particle kinetics in these systems are discussed. Conclusions are drawn in Section 4.

* Corresponding author. Fax: +82 54 279 2903.
E-mail address: jkl@postech.ac.kr (J.K. Lee).
[1] Plenary Speaker at Conf. on Computational Phys. in Brazil (Aug. 4–9, 2008).

0010-4655/$ – see front matter
doi:10.1016/j.cpc.2009.01.004

2. Numerical models and discharge conditions

2.1. Fluid models

Fluid models describe the plasma in terms of averaged quantities such as density, mean velocity and mean energy. These quantities are calculated by solving the particle, momentum and energy conservation equations, which are the first three velocity moments of the Boltzmann equation [14,15]. Poisson's equation is coupled with these fluid equations to obtain the self-consistent electric field. The continuity (particle conservation) equation is solved for the electrons and ions to obtain the particle density. In this study instead of solving the momentum equation, the simpler drift-diffusion approximation is used [16]. This is appropriate when the particles' inertia is negligible as it is the case in most atmospheric-pressure discharges (collision frequency $\nu \gg$ driving frequency ω) [17–19]. The energy equation is solved for the electrons but not for the ions because the latter are assumed to remain at the same temperature as the neutral gas. The average collision frequencies (e.g., ionization and momentum transfer frequencies) and transport coefficients (e.g., source term, diffusion constant, mobility, etc.) used in the equations need to be calculated assuming a velocity or energy distribution function for each species [12,20]. This assumption gives rise to the main limitation of fluid models and the reliability of the simulation results depends on the validity of the assumed distribution function. In the fluid model used in this study, the distribution function is assumed to be Maxwellian. This implies that collisions between particles of the same species are more frequent than any other processes. Although as it is shown later in Section 3 this assumption is not strictly correct, it has been successfully used in many studies of atmospheric-pressure discharges [3,5,8,9,12]. Assuming the distribution to be Maxwellian allows for the transport coefficients and collision frequencies to be expressed as a function of the particle mean energy (temperature), which is determined by solving the energy balance equation. The resulting set of fluid equations are solved numerically by converting the set of coupled differential equations into a set of finite difference equations using the Scharfetter–Gummel scheme [21].

2.2. PIC-MCC models

Instead of assuming a certain velocity distribution function, PIC-MCC simulations represent the actual distribution of each species by a large number of particles that are tracked solving the Newton–Lorentz and Maxwell's equations [19]. In this work the Maxwell equations are substituted by Poisson's equation, i.e. the electrostatic approximation is used. This method does not make any assumption on the distribution function, and provided that the number of particles is sufficiently large, PIC-MCC simulations are able to capture the actual EEPF. Typically, electrons and ions are considered in the model, and neutral gas density is assumed to be uniformly distributed in space. Boundary conditions can also be consistently considered and each collision is modeled by taking into account the velocity of the colliding particles [22]. Elastic, excitation and ionization electron–neutral collisions, and scattering and charge exchange ion–neutral collisions are considered in the model. Coulomb collisions are not included due to computational constraints and their effect shall be subject of future studies. Although Coulomb collisions tend to Maxwellize the electron distribution function, their influence is not expected to change the qualitative picture presented in this manuscript (e.g., at 3 eV Coulomb collisions are much less frequent than electron–neutral collisions at atmospheric pressure) [23]. Although PIC simulations can capture nonlocal effects often encountered in low-temperature plasmas, tracking individual particles is computationally very expensive [24,25]. As a result the number of species that can be modeled is limited and in this study only electrons and singly charged positive ions have been considered.

2.3. Simulation conditions

The study considers DC, RF and microwave atmospheric-pressure helium plasmas sustained by two different sources. The first source consists of two parallel plate electrodes that are separated by a 200 μm gap as shown schematically in Fig. 1(a). The second plasma source is a plasma needle. In this source the electrodes are asymmetric with the ground electrode having an area much larger than the area of the needle itself. This asymmetry

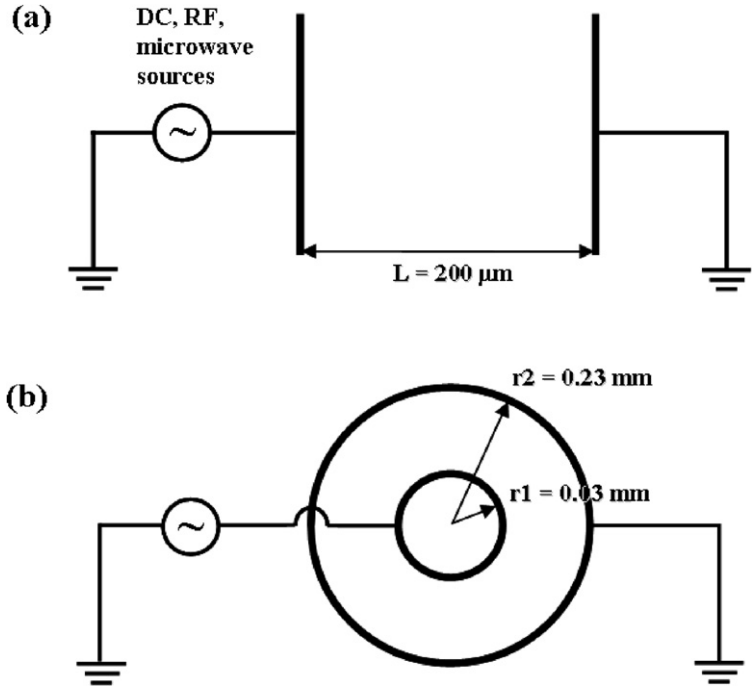

Fig. 1. Schematic diagrams of various plasma sources. (a) Symmetrical; (b) cylindrical current- or voltage-driven discharge.

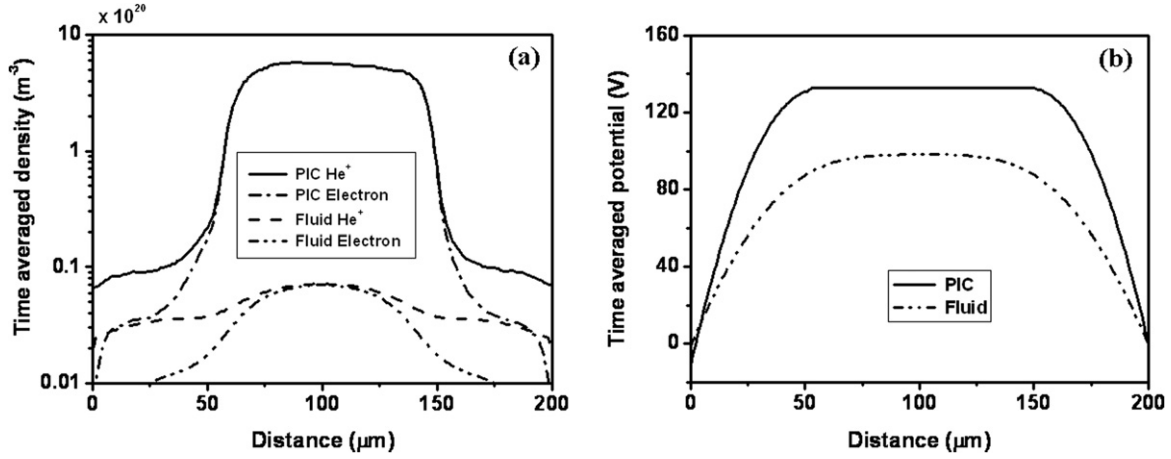

Fig. 2. Comparison of fluid and PIC-MCC simulation results in an RF helium discharge at atmospheric pressure. (a) Time-averaged plasma densities; (b) time-averaged potential profiles.

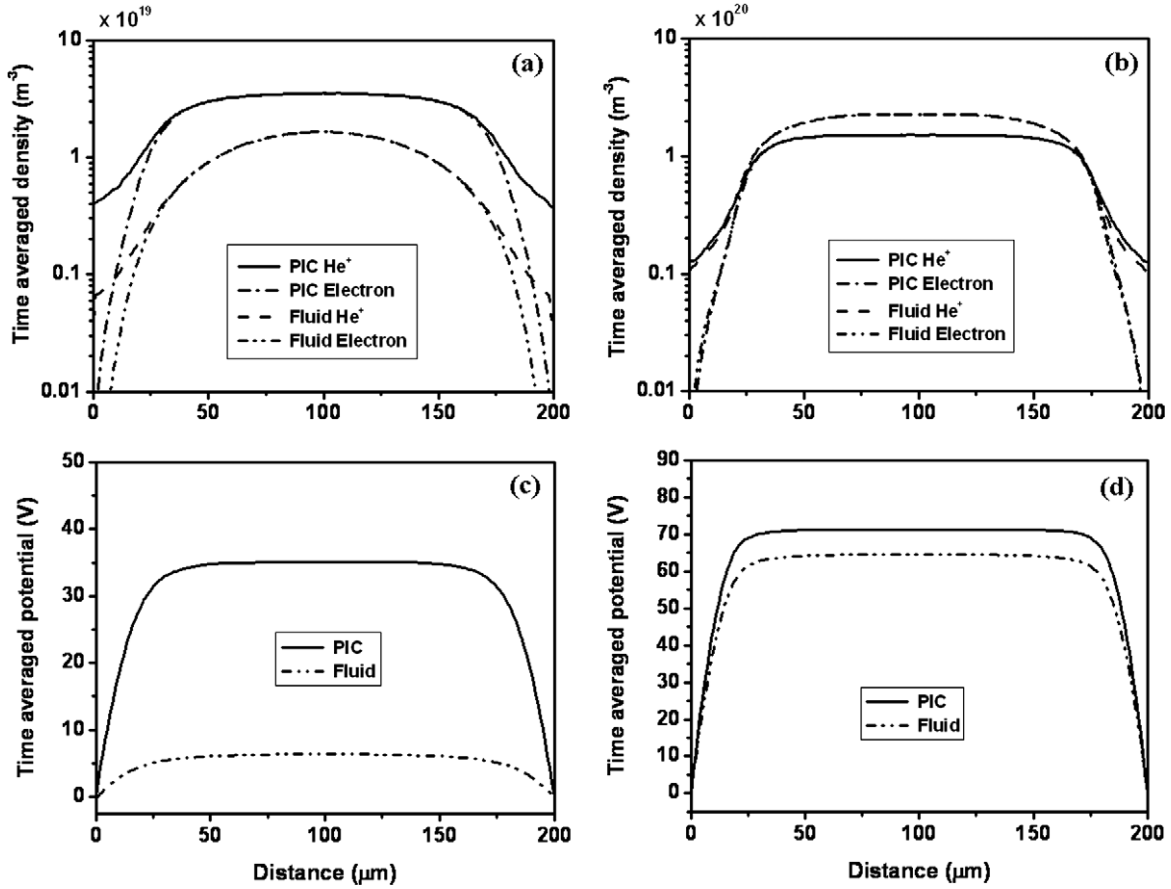

Fig. 3. Comparison between fluid and PIC-MCC simulation results of microwave helium discharges at atmospheric pressure driven by a (a), (c) current source; (b), (d) voltage source. The best correspondence is obtained for the voltage-driven case.

can be captured in a one-dimensional simulation using the coaxial configuration shown in Fig. 1(b). The inner electrode is designed to be 60 μm in diameter and be powered by DC, RF (13.56 MHz) and microwave (2.45 GHz) sources. The voltage (current) value of the power source is chosen to be 1.5 times the minimum sustain voltage (current) required to ignite the discharge. The grounded outer electrode has a radius of 230 μm, resulting in an aspect ratio of ∼8. For stability and accuracy of the simulations, we use a time step Δt of (1–5) $\times 10^{-14}$ s and 200 spatial cells ($\Delta x \sim 1$ μm) [12, 26]. The density at the beginning of the simulations is 10^{17} m^{-3} and the number of physical particles per computer super-particle in the PIC-MCC simulation is rescaled to keep the number of super-particles as low as possible (100–1000 particles per cell). In order to facilitate the comparison with fluid models, a constant ion-induced secondary electron emission coefficient of 0.1 is used in the study.

3. Results and discussion

3.1. Comparison of fluid and PIC-MCC model in symmetrical discharges

For a DC discharge, the potential, density and effective electron temperature profiles obtained by means of PIC-MCC simulations

were already compared with those obtained using fluid models as cited in [7,9]. The simulation conditions were the same in both cases and corresponded to a 200 μm DC helium microplasma operated at atmospheric pressure. Although the electron temperature predicted by the PIC-MCC model is significantly lower than that predicted by the fluid model, a rough qualitative agreement was obtained between both simulation techniques.

Fig. 2 shows the time-averaged density and potential profiles for an RF atmospheric-pressure helium discharge, and compares them with those obtained with the fluid model. A 13.56 MHz–0.8 A/cm^2 root-mean-square (rms) current source is used to sustain the discharges. The shape of density and potential profiles are comparable in both cases, although the peak densities predicted by fluid model (7.1×10^{18} m^{-3}) is much lower than those predicted by PIC-MCC simulations (5.7×10^{20} m^{-3}). This discrepancy is attributed to the assumption of a Maxwellian velocity distribution in the fluid model. The self-consistent EEPF obtained in the PIC simulation is clearly not Maxwellian (Fig. 4(a)). It consists of a large number of low-energy electrons trapped in the bulk plasma, mid-energy electrons with significantly larger temperature and a high-energy tail due to avalanches in the sheaths that originate with secondary electrons [4]. Low energy electrons in the EEPF from the PIC-MCC simulation cause the difference in the density profiles obtained with fluid and PIC-MCC models (Fig. 2).

Finally, the time-averaged profiles of a microwave discharge operated at atmospheric pressure are presented in Fig. 3. Two cases are considered. The first one uses a current source at 10 A/cm^2–2.45 GHz and the second one a voltage source of 135 V–2.45 GHz. Although some differences can also be observed between fluid and PIC simulation results, the order of magnitude and trends obtained with the fluid model are in good agreement with the PIC-MCC simulation results. The best correspondence is obtained for the voltage-driven case, illustrated in Figs. 3(b) and 3(d).

The electron and ion kinetics in atmospheric-pressure plasmas can aid in revealing the physics governing these discharges. Since a fundamental understanding of the plasma physics is required in order to optimize plasma sources for a given application, understanding the formation of the EEPFs in various plasma sources is important. This information is available in PIC-MCC simulations.

As already discussed, three electron groups can be identified in RF microdischarges [6]. The EEPFs in the center of the 200 μm discharge is shown in Fig. 4(a). The energy relaxation length of low-energy electrons is comparable to the width of the potential well experienced by these electrons and a kinetic treatment, such as a PIC-MCC model, is therefore needed to account for the nonlocal kinetics of the low energy electrons. A large number of low-energy electrons with energy less than ∼2 eV are trapped by the ambipolar potential during the RF cycle and they remain with low temperature because the applied RF field is effectively shielded by the sheaths. The high-energy electrons in the bulk plasma result from the acceleration of electrons in the sheaths. Electrons accelerated in the high electric fields of the sheaths gain high energy and gradually lose it in collisions as they transit through the bulk, populating the mid and high energy regions of the EEPF. At atmospheric pressure, the required length for high-energy electrons to lose most of their energy (energy relaxation length) is very small and even in a 200 μm discharge virtually no energetic electron reaches the center of the discharge (Fig. 4(a)). Significant number were observed, however, in a smaller discharge [6, 27]. Since the electron relaxation time in helium RF discharges operated at atmospheric pressure (∼5 ps–10 ns – Fig. 4(b)) is much shorter than the RF period, the electron energy distribution function is strongly time modulated by the driving frequency. When the frequency is increased, the voltage drop across the sheaths reduces, making the source more efficient in delivering the power to the electrons (Fig. 4(c)). Due to the increase in the ratio of the electric field experienced by electrons in the bulk plasma to the electric field in the sheaths [4], the temperature of the low-energy electrons increases with frequency. As a result the EEPF in the discharges driven at microwave becomes closer to a Maxwellian distribution (Fig. 4(a)), and therefore the fluid model is able to better reproduce the PIC-MCC results. It is noted, however, that the improved energy transfer to the electrons with higher driv-

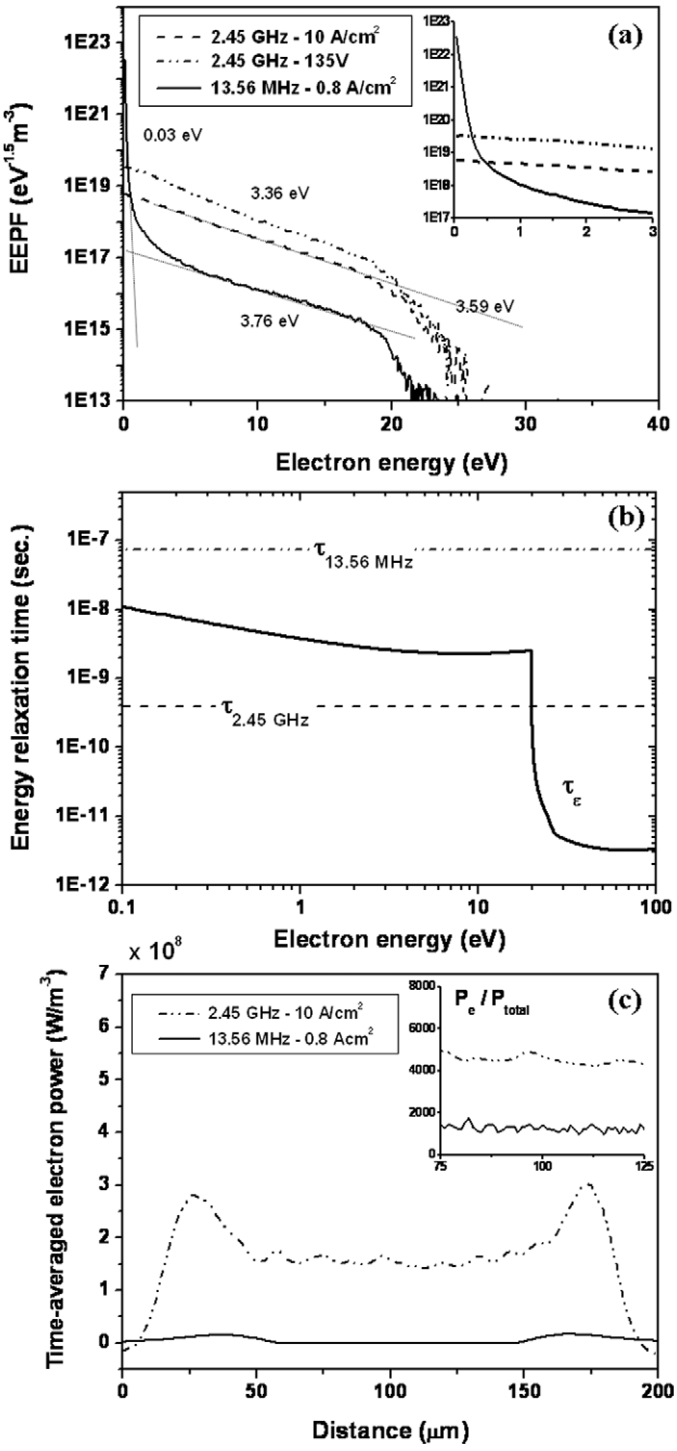

Fig. 4. (a) EEPFs in the center of the discharge; (b) Comparison between the electron energy relaxation time (τ_ε) and the periods ($\tau_{13.56\ \mathrm{MHz}}$ and $\tau_{2.45\ \mathrm{GHz}}$); (c) The spatial profiles of the power deposited to the electrons (P_e) and normalized electron power (P_e/P_{total}) in the bulk.

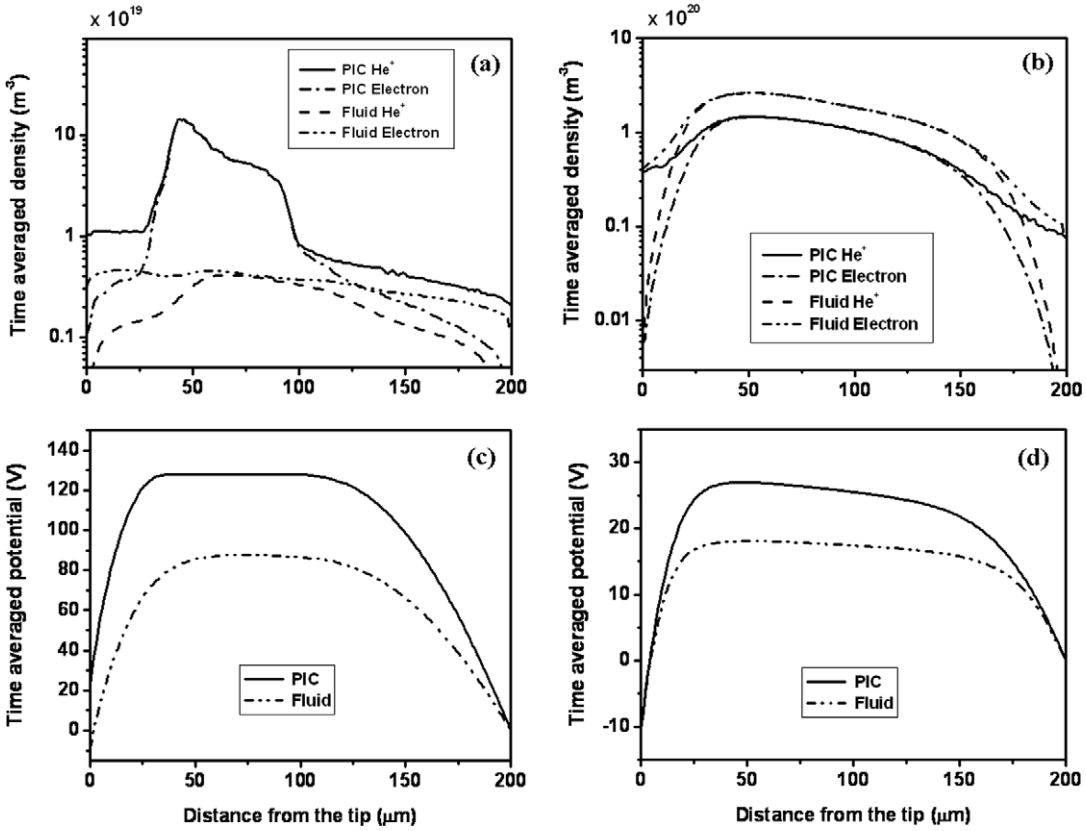

Fig. 5. Comparison between fluid and PIC-MCC simulation results of (a), (c) RF (13.56 MHz – 1.6 A/cm^2 rms); (b), (d) microwave (2.45 GHz – 15 A/cm^2 rms) helium discharges at atmospheric pressure.

ing frequency does not always lead to higher plasma density [28,29].

3.2. Comparison of fluid and PIC-MCC model in asymmetric discharges

Time-averaged density and potential profiles as a function of the distance from the tip of a plasma needle (inner conductor in Fig. 1(b)) to the ground electrode (outer conductor) are shown in Fig. 5 for atmospheric-pressure helium discharges driven at 13.56 MHz and 2.45 GHz. As a result of the higher electric field in the proximity of the inner electrode, the density profiles are asymmetric and the maxima are shifted to a position closer to the smaller electrode. As for the parallel plate symmetrical case (Fig. 3), the best agreement between fluid and PIC-MCC simulation results is obtained when the discharges are driven at microwave frequency (Figs. 5(b) and 5(d)).

The time-averaged power absorption profiles predicted by the fluid and PIC-MCC simulation models agree reasonably well among them (Fig. 6(a)), and both simulations indicate that the power delivered to the ions is mainly dissipated near the inner electrode. This contrasts with much broader region where the input power is absorbed by the electrons. The change of EEPFs in cylindrical discharges operated at atmospheric pressure with driving frequency is similar to that in symmetrical discharges, as illustrated in Figs. 4(a) and 6(b). The employment of higher frequency significantly enhances the performance of the device. Since the sheath potential scales as the square of the frequency [30], the energy deposited to the ions in the sheath region is reduced, therefore, microwave plasmas are more efficient in coupling power to the electrons and have longer lifetimes due to the reduction of the damage caused by the ion bombardment on the electrodes (Fig. 6(c)).

4. Conclusion

DC, RF and microwave helium discharges operating at atmospheric pressure have been simulated using fluid and PIC-MCC computational models. PIC-MCC results reveal that the electron energy distribution function is far from thermodynamic equilibrium despite the large collisionality encountered at atmospheric pressure. Thus, the information predicted by fluid models that assume a Maxwellian velocity distribution function is questionable. Although this difference can affect the reliability of fluid simulations, fluid models offer a computationally efficient mean to analyze these discharges obtaining a qualitative agreement in many circumstances. It is found that this agreement is better when the discharges are operated at microwave frequencies due to better approximation of the EEPF.

PIC-MCC results indicate that the EEPF evolves from a three-temperature to a Druyvesteyn-like distribution as the driving frequency increases from 13.56 MHz to 2.45 GHz in both the symmetric and asymmetric discharges. This transition is due to a change in the power deposition profile. As frequency increases, the fraction of power coupled to the electrons in the bulk increases, heating the electrons trapped by the ambipolar field and shifting the EEPF toward a Druyvesteyn-like distribution. Despite the relatively large sheath voltages, frequent ion–neutral collisions reduced the maximum energy acquired by the ions as they transit the sheath and the average ion energy at the electrodes of a plasma needle is found to be less than 1 eV.

It is concluded that the numerical techniques can complement experimental diagnostics and help to develop a better understanding of the physics governing low-temperature atmospheric-pressure plasmas. This understanding will facilitate the develop-

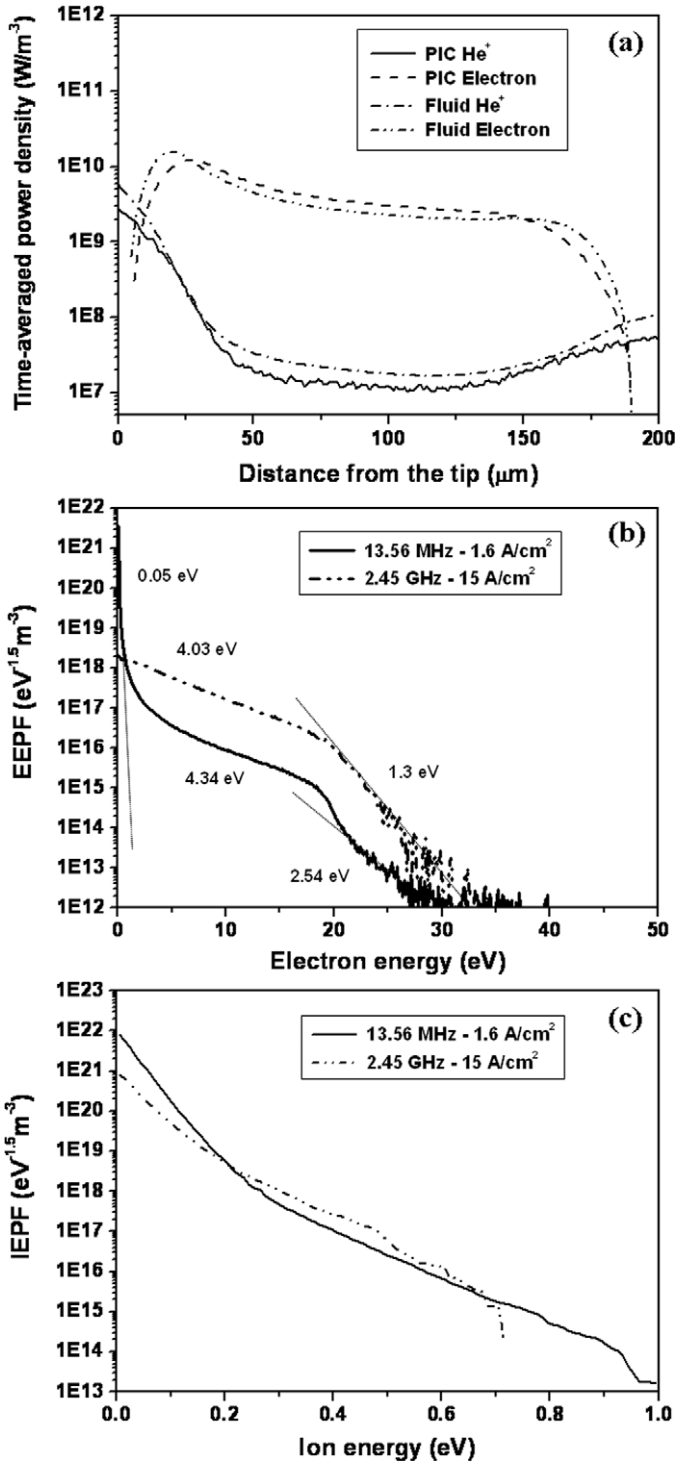

Fig. 6. (a) Time-averaged profiles of the power delivered at current density of 15 A/cm^2 rms in cylindrical microwave discharge; (b) Electron energy probability functions in the bulk plasma; (c) Ion energy probability functions in the sheath region.

ment of more efficient devices and the use of plasmas in even more promising tasks.

Acknowledgements

This work was supported in part by the Korea Science and Engineering Foundation (KOSEF) grant funded by the Korea government (MOST) (No. R01-2007-000-10730-0) and the Korea Ministry of Education, Science and Technology through its Brain Korea 21 program.

References

[1] K.H. Becker, K.H. Schoenbach, J.G. Eden, J. Phys. D: Appl. Phys. 39 (2006) R55–R70.
[2] G. Fridman, A. Shereshevsky, M.M. Jost, A.D. Brooks, A. Fridman, A. Gutsol, V. Vasilets, G. Friedman, Plasma Chem. Plasma Process. 27 (2007) 163–176.
[3] J.J. Shi, M.G. Kong, Phys. Rev. Lett. 96 (2006) 105009.
[4] F. Iza, G.J. Kim, S.M. Lee, J.K. Lee, J.L. Walsh, Y.T. Zhang, M.G. Kong, Plasma Processes and Polymers 5 (2008) 322–344.
[5] Q. Wang, I. Koleva, V.M. Donnelly, D.J. Economou, J. Phys. D: Appl. Phys. 38 (2005) 1690–1697.
[6] F. Iza, J.K. Lee, M.G. Kong, Phys. Rev. Lett. 99 (2007) 075004.
[7] J. Choi, F. Iza, J.K. Lee, C.M. Ryu, IEEE Trans. Plasma Sci. 35 (2007) 1274–1278.
[8] M.J. Kushner, J. Appl. Phys. 95 (2006) 846–859.
[9] Q. Wang, D.J. Economou, V.M. Donnelly, J. Appl. Phys. 100 (2006) 023301.
[10] Y. Sakiyama, D.B. Graves, J. Appl. Phys. 101 (2007) 073306.
[11] Z. Donko, P. Hartmann, K. Kutasi, Plasma Sources Sci. Technol. 15 (2006) 178–186.
[12] H.C. Kim, F. Iza, S.S. Yang, M. Radmilovic-Radjenovic, J.K. Lee, J. Phys. D: Appl. Phys. 38 (2005) R283–R301.
[13] Y.J. Hong, S.M. Lee, G.C. Kim, J.K. Lee, Plasma Processes and Polymers 5 (2008) 583–592.
[14] T. Makabe, Advances in Low Temperature RF Plasmas: Basis for Process Design, Elsevier, Amsterdam, 2002.
[15] F.F. Chen, J.P. Chang, Lecture Notes on Principles of Plasma Processing, Kluwer Academic/Plenum Publishers, New York, 2003.
[16] J.P. Boeuf, Phys. Rev. A 36 (1987) 2782.
[17] D.B. Graves, J. Appl. Phys. 62 (1987) 88–94.
[18] S.K. Park, D.J. Economou, J. Appl. Phys. 68 (1990) 3904–3915.
[19] T. Makabe, N. Nakano, Y. Yamaguchi, Phys. Rev. A 45 (1992) 2520–2531.
[20] The Siglo Database, Kinema Research & Software, http://www.kinema.com/.
[21] D.L. Scharfetter, H.K. Gummel, IEEE Trans. Electron Devices 16 (1969) 64–77.
[22] J.P. Verboncoeur, M.V. Alves, V. Vahedi, C.K. Birdsall, J. Comput. Phys. 104 (1993) 321–328.
[23] Y.P. Raizer, Gas Discharge Physics, Springer, Berlin, 1991.
[24] G.Y. Park, S.J. You, F. Iza, J.K. Lee, Phys. Rev. Lett. 98 (2007) 085003.
[25] H.C. Kim, J.K. Lee, Phys. Rev. Lett. 93 (2004) 085003.
[26] C.K. Birdsall, IEEE Trans. Plasma Sci. 19 (1991) 65.
[27] G.J. Kim, F. Iza, J.K. Lee, J. Phys. D: Appl. Phys. 39 (2006) 4386–4392.
[28] S.K. Ahn, S.J. You, H.Y. Chang, Appl. Phys. Lett. 89 (2006) 161506.
[29] D.W. Liu, F. Iza, M.G. Kong, Appl. Phys. Lett. 93 (2008) 261503.
[30] M.A. Lieberman, A.J. Lichtenberg, Principles of Plasma Discharges and Material Processing, John Wiley & Sons Inc., New York, 2005.